[6]Wygnanski, I. and Fiedler, H. E., "Some Measurements in the Self-Preserving Jet," *Journal of Fluid Mechanics*, Vol. 38, 1969, pp. 577-612.

[7]Harch, W. H., "An Experimental Investigation Into the Velocity Field and Aerodynamic Noise Sources of an Unheated Fully Pulsed Air Jet," Ph.D. Thesis, University of Queensland, St. Lucia, Brisbane, Australia, 1977.

[8]Wygnanski, I. and Fiedler, H. W., "The Two-Dimensional Mixing Region," *Journal of Fluid Mechanics*, Vol. 41, 1970, pp. 327-361.

Resonance Refractivity Studies of Sodium Vapor for Enhanced Flow Visualization

G. Blendstrup* and D. Bershader†
Stanford University, Stanford, Calif.
and
P.W. Langhoff‡
Indiana University, Bloomington, Ind.

Introduction

REFRACTIVE methods pioneered by the studies of Mach, Zehnder, Toepler, and others have been used for about 100 years to visualize fluid-dynamic flow phenomena. While there have been new developments in sophistication of the optical methodology and instrumentation, the sensitivity of essentially all work to date has been controlled by the specific refractivity of diatomic gases, e.g., air, in the visible portion of the spectrum. That quantity, K_0, appears in the well-known Dale-Gladstone constitutive relation[1]

$$n-1=K_0\rho \tag{1}$$

relating refractive index n and gas density ρ. Its value is relatively constant over the visible portion of the spectrum:

$$K_{0_{\text{air}}} \approx 2.3\times 10^{-4}\ \text{m}^3/\text{kg}$$

The relatively small magnitude of $K_{0_{\text{air}}}$ has largely limited the application of techniques such as interferometry, Schlieren, and shadowgraphy to compressible flows with substantial density gradients; or to free convective flows with sizable thermal gradients. As an example, the density change corresponding to 0.1 fringe shift in a test rig with a transverse light path of 10 cm is 2.2×10^{-3} kg/m^3 or 0.17% of standard atmospheric density. It turns out that a substantially higher sensitivity is desirable for several applications of current interest. These include vortices and turbulence in low-speed flow, propagation of sound or noise in the audible range, rarified gas flow, and meteorological flows.

The idea of using a tunable narrow band dye laser to illuminate a gas near its resonance line in order to increase the effective Dale-Gladstone "constant" was discussed in an earlier paper by two of the present authors.[2] Since the resonance transitions of air and other diatomic gases lie in the far ultraviolet, the work just referred to as well as the present Note deals with the resonance refractivity of sodium vapor. In a laboratory application of this method, the working fluid would be seeded with small quantities of sodium vapor or other suitable material, probably in the range 10^{-4} to 10^{-3} mole fraction.

The present Note describes recent results, including refinement of both the theoretical calculations and the experimental setup to check the resonance dispersion of sodium vapor, as well as the final calibration experiment on sodium vapor refractivity.

Theoretical

Atomic absorption and dispersion line shapes under conditions of Doppler, collision, and natural broadening can be represented by Voigt profiles of the form[3]

$$n_r(\nu)-1=\frac{\sqrt{\ell n 2}}{8\pi^2\sqrt{\pi}}\cdot\frac{e^2Nf_r}{mc\epsilon_0\gamma_D\nu_r}\int_{-\infty}^{\infty}\frac{\epsilon-\nu}{(\epsilon-\nu)^2+\gamma_L^2/4}\cdot\exp[-4\,\ell n 2\cdot(\epsilon-\nu_r)^2/\gamma_D^2]\,d\epsilon \tag{2}$$

$$\mu_r(\nu)=\frac{\sqrt{\ell n 2}}{4\pi\sqrt{\pi}}\cdot\frac{e^2Nf_r\gamma_L}{mc\epsilon_0\gamma_D}\int_{-\infty}^{\infty}\frac{1}{(\epsilon-\nu)^2+\gamma_L^2/4}\cdot\exp[-4\ell n 2\cdot(\epsilon-\nu_r)^2/\gamma_D^2]\,d\epsilon \tag{3}$$

where the usual symbols are used for the familiar physical constants. Further, μ is the absorption index, f_r and ν_r are the total integrated oscillator strength of the particular doublet component and the corresponding resonance transition frequency, respectively; and γ_L and γ_D are the Lorentzian and Doppler "full-halfwidths" (full width at half maximum). The Doppler value is

$$\gamma_D=2\frac{\nu_r}{c}\sqrt{\frac{2kT}{M}}\sqrt{\ell n 2} \tag{4}$$

while the Lorentzian value is the sum of natural and collision widths

$$\gamma_L=\gamma_n+\gamma_c \tag{5}$$

Recent measurements of sodium self-broadening over the number density range $N\sim 10^{16}$ to 10^{22} (atoms/m^3) have given the values for the proportionality constant C_r in the relation

$$\gamma_c=2C_rN$$

indicated in Table 1. Table 1 also presents values of oscillator strengths, resonant frequencies and wavelengths, and natural widths for the two sodium D-lines.

By use of dimensionless variables

$$u=\frac{2\sqrt{\ell n 2}(\nu-\nu_r)}{\gamma_D} \tag{6a}$$

$$a=\frac{\gamma_L}{\gamma_D}\sqrt{\ell n 2}\ \text{(Voigt parameter)} \tag{6b}$$

$$y=\frac{2\sqrt{\ell n 2}(\epsilon-\nu_r)}{\gamma_D} \tag{6c}$$

Table 1 Sodium D-lines parameters[a]

	λ_r, Å	ν_r, 10^{14}/s (Ref. 7)	f_r (Ref. 8)	γ_n, 10^6/s (Ref. 8)	C_r, 10^{-15} m^3/s (Ref. 9)
D_1	5895.930	5.083345	0.327	9.99	7.32
D_2	5889.963	5.088500	0.655	10.03	8.59

[a]D_1 refers to the $^2S_{1/2}\rightarrow{}^2P_{1/2}$ transition, whereas D_2 refers to the $^2S_{1/2}\rightarrow{}^2P_{3/2}$ transition.

Received April 18, 1978; revision received June 12, 1978.

Index categories: Experimental Methods of Diagnostics; Lasers.

*Research Assistant, Dept. of Aeronautics and Astronautics. Student Member AIAA.

†Professor, Dept. of Aeronautics and Astronautics. Fellow AIAA.

‡Professor, Department of Chemistry.

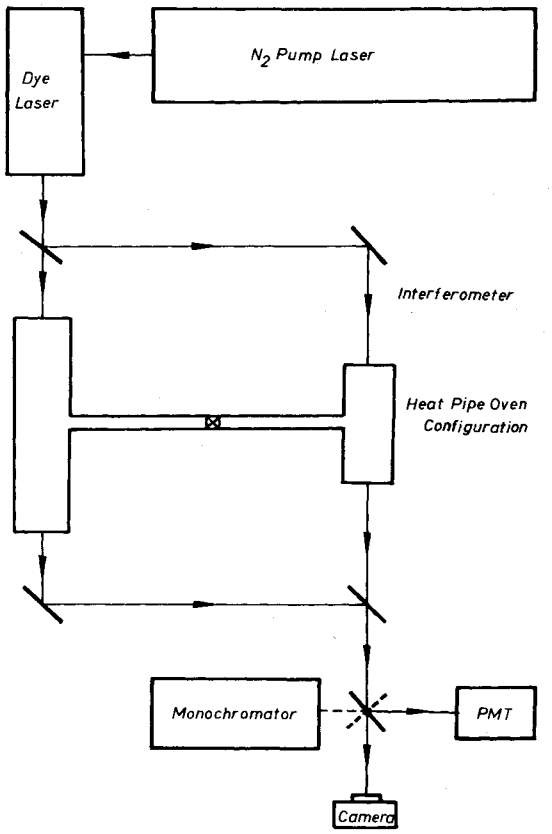

Fig. 1 Schematic diagram of resonant refractivity apparatus.

it is possible to rewrite Eqs. (2) and (3) to read

$$n_r(\nu)-1=\frac{\sqrt{\pi}}{8\pi^2}\frac{e^2Nf_ra}{m\epsilon_0\gamma_L\nu_r}\left[\frac{1}{\pi}\int_{-\infty}^{\infty}\frac{y-u}{a^2+(u-y)^2}e^{-y^2}dy\right] \tag{2a}$$

$$\mu_r(\nu)=\frac{\sqrt{\pi}}{2\pi}\frac{e^2Nf_ra}{m\epsilon_0\gamma_Lc}\left[\frac{a}{\pi}\int_{-\infty}^{\infty}\frac{1}{a^2+(u-y)^2}e^{-y^2}dy\right] \tag{3a}$$

where the entities in square brackets can be recognized as the imaginary and real parts, respectively, of the complementary error function of complex argument

$$W(z)=e^{-z^2}\mathrm{erfc}(-i\cdot z),\quad z=u+ia \tag{7}$$

A computer program was used to calculate the $W(z)$ function based, in turn, on a method of Hummer and Rybicki[3] to calculate the absorption Voigt profile [real part of $W(z)$]. To obtain the imaginary part, the Kroenig-Heisenberg[4] expression was employed relating the real and imaginary parts of $W(z)$ to each other. A plot of the theoretical values of specific refractivity vs wavelength is shown in Fig. 2 (solid line).

Experiment

Major features of the experiment are highlighted in the schematic diagram of Fig. 1. Sodium vapor is generated and contained in a defined configuration by use of the heat-pipe oven apparatus. The latter, in turn, occupies a portion of the path in a Mach-Zehnder interferometer, and changes in sodium refractivity are monitored by fringe shifts. The light source is a tunable dye laser which has suitable resolution near the sodium resonance. The description of the transversely pumped dye laser in Hänsch[5] configuration and the operation of the two heat-pipe ovens was briefly reviewed in Ref. 2. Modifications and refinements required in the more recent work included changing the chromel-alumel thermocouples to more heat-resistant platinel thermocouples, replacing the sapphire windows with fused-silica quartz optical flats of high flatness and parallelism, and enclosing the light beam in the interferometer to eliminate fringe shifts due to ambient air currents.

The dye-laser system itself was mounted together with the nitrogen pump laser (Molectron UV300) on a heavy 1½-in.-thick aluminum plate. Its performance was found to be quite comparable with the Molectron DL22 system, having a repeatability, stability, and accuracy better than 0.1 Å, a bandwidth of 0.2 Å, and a pulse energy of approximately 170 μJ at 5890 Å. The emitted wavelength corresponding to any particular orientation of the grating was calibrated with a MacPherson 1-m-scanning monochromator together with sodium and neon vapor lamps to produce emission lines at 5889.96 and 5852.5 Å, respectively.

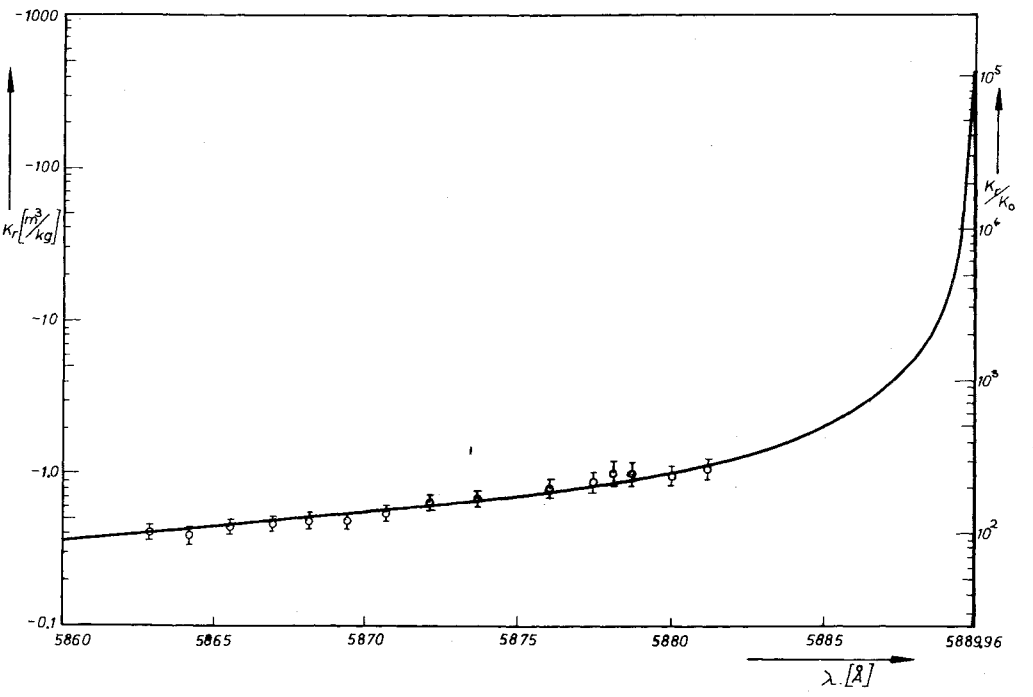

Fig. 2 Resonant dispersion in sodium vapor. Points represent measured values. Negative ordinate values relate to high-frequency-line wing where $n>7$.

Installation of a heater unit with feedback on-off switches made it possible to control the temperatures in the heat-pipe ovens separately to a fraction of a degree Celsius. Holding the temperature in one oven constant and raising or lowering the temperature in the other gave measurable fringe shifts which could then be related to the recorded pressure and density change. Typical fringe-shift studies were carried out in the regime between 440° and 480°C for sodium number density changes of the order of 5×10^{21} m^{-3} corresponding to temperature changes of approximately 10°C.

The fringes were focused on a plate with a pinhole in front of a high-gain photomultiplier tube (RCA C31000F) which was cooled down to −30°C to lower the dark current and increase the signal-to-noise ratio. The output of the PMT was then recorded with an X-Y plotter, monitoring the intensity changes in a typical periodic fashion as the fringes marched across the pinhole.

Results and Discussion

Investigation of the computed absorption and refractivity profiles showed some noteworthy features which were confirmed by the experimental results. The shape of the refractivity curves are highly insensitive to the Voigt parameter a and temperature T, allowing us to write Eq. (1) in the following form

$$n_r(\lambda,T)-1=K_r(\lambda)\rho(T) \tag{1a}$$

where subscript r means near the resonance regime.

Figure 2 shows the graph of the calculated values for $K_r(\lambda)$ which are valid to a high degree of accuracy for a broad temperature range and for λ smaller than 5890 Å. The experimental results in the investigated wavelength range are in good accordance with the theory. As mentioned above, the fringe shifts were measured and then related to the known change of density and effective length of sodium column according to

$$S\cdot\lambda_0=K_r(\lambda)(\rho_1\ell_1-\rho_2\ell_2) \tag{8}$$

where S denotes the fringe shift, λ_0 the wavelength of the dye laser, and $\rho_{1,2}$ and $\ell_{1,2}$ the mass density and length of the sodium column before and after the temperature change, respectively.

The maximum refractivity enhancement was limited by the resonance absorption of the approximately 0.5-m-long sodium column. At about 7 Å away from resonance and $T=465$°C the absorption coefficient of $\mu\approx7$ m^{-1} makes it virtually impossible to measure fringe shifts even closer to resonance. Nevertheless, the relatively gentle slope of the dispersion curve enables us to achieve enhancements in the wings which are of the order of 200 to 300 compared to the zero-frequency Dale-Gladstone constant $K_{0_{Na}}=4.051\times10^{-3}$ m^3/kg of sodium. If compared with the nonresonant value of air $K_{0_{air}}\approx2.3\times10^{-4}$ m^3/kg the resonance refractivity enhancement reaches a value of 5.0×10^3.

Furthermore, the relative magnitude of the absorption line shape in the wings is proportional to the Lorentzian line width, whereas (as mentioned above) the refractivity line shape is quite insensitive to a [see Eq. (6b)] and any change of γ_L. Therefore, any decrease of γ_L would make it possible to go closer to the resonance line and to utilize a larger index of refraction.

In this respect the resonant refractivity technique for seeded flow-field visualization looks quite promising. The collision linewidth for sodium in the presence of an inert buffer gas like argon, which behaves quite similarly to nitrogen and air, is over 25 times smaller than in the present case with sodium-sodium collisions. Assuming the same maximum tolerable absorption and the same length of sodium column it should be possible to make use of an enhanced specific refractivity significantly larger than in the case of sodium self-broadening.

Acknowledgment

This work was supported by the Air Force Office of Scientific Research, Department of Defense, under Contract AFOSR 74-2670A.

References

[1]Van Vleck, J., *Electric and Magnetic Susceptibilities,* Oxford University Press, 1932.

[2]Bershader, D., Prakash, S. G., and Huhn, G., "Improved Flow Visualization by Use of Resonant Refractivity," AIAA Paper 76-71, Washington, D.C., Jan. 1976.

[3]Hummer, D. G., *Memoirs of the Royal Astronomical Society,* Vol. 70, 1965, p. 1.

[4]Nussenzweig, H. M., *Causality and Dispersion Relations,* Academic Press, New York, 1972.

[5]Hänsch, T. W., "Applications of Dye Lasers," *Dye Laser,* edited by F. Schaefer, Springer, New York, 1973.

[6]McCartan, D. G. and Farr, J. M., *Journal of Physics,* Vol. B9, June 1976, p. 985.

[7]Moore, C. E., "Atomic Energy Levels," National Bureau of Standards Circular 467, Vols. 1, 2, and 3, 1949.

[8]Wiese, W. L., Smith, M. W., and Miles, B. M., "Atomic Transition Probabilities," Natl. Standard Reference Data Service, 22, Vol. 22, 1969.

[9]Niemax, K. and Pichler, G., *Journal of Physics,* Vol. B8, Feb. 1975, p. 179.

Chemical Equilibrium Compositions of Hydrogen-Oxygen-Nitrogen Systems

Frank Thiele*
Technische Universität, Berlin, West Germany

Chemical Equilibrium Formulation

THE prediction of hydrogen-air diffusion flames (see, e.g., Ref. 1) has focused interest in solution techniques for the calculation of chemical equilibrium compositions. The technique presented here is based on the method of equilibrium constants, which is stated below.

Because of low pressures and high temperatures in flames, the theory of thermally perfect gases can be applied. Thus we consider the perfect gas mixture of nine species (H_2, O_2, H, O, OH, H_2O, N_2, N, NO; $i=1,\ldots,N$). These species consist of three elements (H, O, N; $j=1,\ldots,E$). The element fractions $\tilde{Y}_j$ can be written as

$$\text{H:}\quad \tilde{Y}_1=\tilde{W}_1(2Z_1+Z_3+Z_5+2Z_6) \tag{1}$$

$$\text{O:}\quad \tilde{Y}_2=\tilde{W}_2(2Z_2+Z_4+Z_5+Z_6+Z_9) \tag{2}$$

$$\text{N:}\quad \tilde{Y}_3=\tilde{W}_3(2Z_7+Z_8+Z_9) \tag{3}$$

where the abbreviation $Z_i=Y_i/W_i$ has been used. Y_i and W_i are the mass fraction and the molecular weight of the ith species, respectively, and $\tilde{W}_j$ is the atomic weight of the jth element.

Received Jan. 27, 1978; revision received June 30, 1978.

Index categories: Thermochemistry and Chemical Kinetics; Reactive Flows.

*Research Scientist, Hermann-Föttinger-Institut für Thermo- und Fluiddynamik.